Final Report

A STUDY OF LOW-NOISE BROADBAND VLF RECEIVING TECHNIQUES

By: L. H. RORDEN

Prepared for:

U.S. NAVAL RESEARCH LABORATORIES
WASHINGTON 25, D.C.

CONTRACT Nonr 3249 (00)X

STANFORD RESEARCH INSTITUTE

MENLO PARK, CALIFORNIA

STANFORD RESEARCH INSTITUTE
MENLO PARK CALIFORNIA

September 1965

Final Report

A STUDY OF LOW-NOISE BROADBAND VLF RECEIVING TECHNIQUES

Prepared for:

U.S. NAVAL RESEARCH LABORATORIES
WASHINGTON 25, D.C.

CONTRACT Nonr 3249 (00)X

By: L. H. RORDEN

SRI Project 3333

Approved: W. R. VINCENT, MANAGER
COMMUNICATION LABORATORY

D. R. SCHEUCH, EXECUTIVE DIRECTOR
ELECTRONICS AND RADIO SCIENCES

Copy No. 6

ABSTRACT

The basic difficulty in optimizing the noise performance of receiving systems which must use an electrically small antenna is the lack of a complete noise theory for a reactive source. This report has attempted to add to this theory in three areas:

First, the various types of small antennas have been put on a common basis of comparison. The parameters of effective length, effective area, effective volume, and intrinsic bandwidth have been defined for antennas sensitive to electric fields and for those sensitive to magnetic fields. These parameters have been evaluated for a number of common antenna structures.

Second, a general method of describing the noise performance of any amplifier has been developed in both of its dual forms. This particular characterization, based on complex-correlated input noise voltage and current generators, was chosen out of many possibilities because it is easily applied to the problem of determining noise performance with an arbitrary source. These noise parameters have been evaluated for several types of amplifying devices.

Third, the ultimate theoretical limits on sensitivity have been explored, and a general method of determining the bounds, in terms of the parameters introduced in the previous sections, has been developed. These bounds have been evaluated in several examples.

CONTENTS

ILLUSTRATIONS

TABLES

1. INTRODUCTION

The continual demand for better communications, detection systems, low-noise amplifiers, and related applications has prompted a good deal of research into the causes and effects of noise in physical devices. This is particularly true in the field of electronics, where inherent device noise sets fundamental limits to the system performance that can be obtained. As a result, the sources of noise are well understood, and they have been thoroughly treated by such authors as van der Ziel [1954],* and the general theory of networks containing noise sources has been well developed by such authors as Haus and Adler [1959].

The purpose of this investigation has been to extend and apply these theories to the description and optimization of the performance of VLF receiving systems. This subject, and in fact the entire more general problem of noise performance with source impedances that are inherently reactive or cannot be transformed to the optimum impedance, has apparently received little attention in the literature. This report, therefore, undertakes the description of the properties of antennas pertinent to the subject, the development of a complete noise characterization of the amplifying devices generally used, and the analysis and comparison of performances of various systems. Although some of the expressions derived are of a very general nature, no attempt has been made to apply them except to the case at hand.

* References are given at the end of the report.

BLANK PAGE

2. SMALL ANTENNAS

In virtually all applications involving reception of electromagnetic waves at frequencies below about 1 MHz it is impractical and generally unnecessary to construct antennas of resonant dimensions. The "electrically small" antennas used at these frequencies are generally satisfactory for reception in spite of their poor efficiency because of the existing high noise levels. Shelkunoff and Friis [1952] are referenced for a complete discussion of "electrically small" and "electrically short" antennas.

Antennas of resonant dimensions couple the propagating wave to the antenna circuit, allowing power transfer at nearly 100 percent efficiency. This type of antenna can be characterized by several parameters such as directivity, capture area, and terminal impedance. Since the terminal impedance can be made to approach the pure radiation resistance over almost arbitrarily large bandwidths, by using structures such as log periodics, antennas of this type can deliver power efficiently to broadband preamplifiers. Electrically small antennas, on the other hand, couple either to the electric or to the magnetic components of the field, and do not depend upon the phase delay attendant with propagating power. Such antennas can be characterized by the directivity of a small dipole, and impedance which is predominantly reactive, being capacitive for antennas that are sensitive to electric fields and inductive for antennas sensitive to magnetic fields. In either case, the radiation resistance is generally so small that it is negligible in comparison with the loss resistance of the antenna and its matching network. Any lossless small antenna, regardless of its type or size, has a capture area A_c given by

$$A_c = \frac{P_a}{|\vec{P}|} \leq \frac{3\lambda^2}{8\pi} \qquad (2.1)$$

where P_a is the available power at the antenna terminals, vector $\vec{P}$ is the power per unit area of the wave, and λ is the wave length. P_a, or more generally P_e—the exchangeable power introduced by Haus and Adler [1959]—is the maximum power that can be delivered to a conjugate match, assuming the only resistance in the antenna circuit is the radiation resistance.

The inequality in Eq. (2.1) is due to the fact that the available power is a function of the polarization and direction of the wave with respect to the antenna.

In practice, the available power cannot be obtained because the antenna and its matching network are generally lossy, and also because the high antenna reactance generally limits the bandwidth over which an effective match can be made with a simple network. For these reasons, the capture area is not considered a useful measure of the performance of a small antenna. A parameter which has been found far more useful is the "effective volume," S, defined as the ratio of energy stored in the antenna reactance to the energy per unit volume in the corresponding field of the incident wave. Consider, for example, a "plate" antenna such as that shown in Fig. 2.1(a), which consists of two conducting plates of dimensions a by b, and separated by distance d. An electric field E normal to the plates will induce an open circuit voltage

$$V_0 = Ed \quad . \tag{2.2}$$

By the usual definition, the "effective length" is

$$l_e \doteq \frac{V_0}{E} = d \quad . \tag{2.3}$$

The existence of the normal electric field and its associated displacement flux D induces a surface charge density

$$\sigma = D = \epsilon E \quad , \tag{2.4}$$

where ϵ is the permittivity of the surrounding medium. The short circuit current due to the field will then be

$$I_s = \frac{d}{dt} \int_A \sigma dA$$

$$= j\omega \epsilon E a b \qquad a >> d;\ b >> d \ , \tag{2.5}$$

where A is the area of one plate, neglecting fringing, and ω is the angular wave frequency. For convenience, the capital letters used to denote fields,

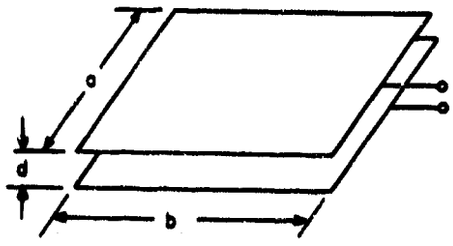

(a) RECTANGULAR PLATES

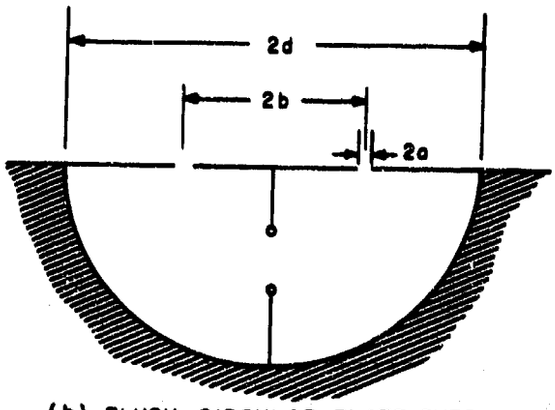

(b) FLUSH CIRCULAR PLATE OVER HEMISPHERICAL CAVITY (CROSS SECTION)

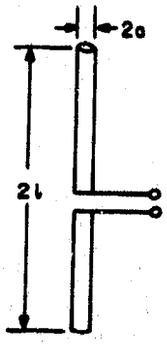

(c) CYLINDRICAL DIPOLE

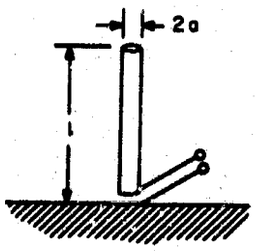

(d) CYLINDRICAL MONOPOLE

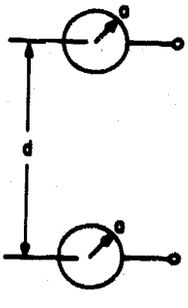

(e) SPHERES

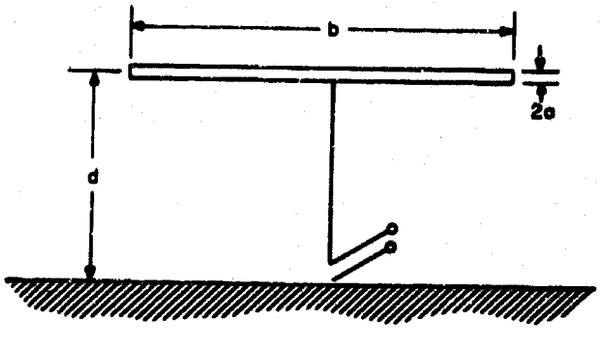

(f) T

D-3383-1

FIG. 2.1 CAPACITIVE ANTENNAS

voltages, and currents will be considered rms values of single frequency signals or of noise in a specified bandwidth, and in general will be considered functions of frequency.

The ratio of short circuit current to the rate of change of displacement flux yields an "effective area"

$$A_e \triangleq \frac{I_s}{j\omega D} = ab \quad , \tag{2.6}$$

which in this case is equal to the physical area of a plate, neglecting fringing. An exact calculation would show that A_e is somewhat larger than the physical area of a plate. From Thevenin's theorem

$$I_s = V_0 j\omega C_a \quad , \tag{2.7}$$

where C_a is the antenna capacitance. Combining Eqs. (2.2), (2.5), and (2.7)

$$C_a = \frac{\epsilon ab}{d} \quad , \tag{2.8}$$

which agrees with the capacitance calculated by the usual methods.

The peak energy per unit volume in the incident field is

$$\frac{W_f}{S} = \epsilon |E|^2 \quad , \tag{2.9}$$

while the peak energy stored in the antenna is

$$W_c = C_a V_0^2 = \epsilon abd |E|^2 \quad . \tag{2.10}$$

The ratio is the "effective volume" S defined above,

$$S = abd = l_e A_e \quad , \tag{2.11}$$

or more generally

$$S \doteq \frac{|V_0 I_s|}{\omega\epsilon |E|^2} \quad , \tag{2.12}$$

From the above expressions it can also be seen that

$$C_a = \frac{\epsilon A_e}{l_e} \quad . \tag{2.13}$$

Approximate expressions for the effective length, area, and volume for the types of antennas shown in Fig. 2.1 are listed in Table 2.1 on page 11. For different forms or better approximations, consult the methods and formulas given by Shelkunoff and Friis [1952] or Terman [1943].

It is interesting to note that a flush plate antenna such as Fig. 2.1b will produce virtually no distortion of the fields if the gap between plate and ground plane is kept sufficiently small, and if its load impedance, generally the preamplifier input impedance, is essentially a short circuit. Furthermore, the field strength can be accurately calibrated, knowing only the short circuit current and the plate area.

By replacing the electric field and flux with the magnetic field H and flux B where

$$B = \mu H \quad , \tag{2.14}$$

and μ equals the permeability of the medium, a similar set of relations emerges as shown in Table 2.1. Figure 2.2 illustrates several types of magnetic antennas for which the effective length, area, and volume have been tabulated. For other shapes or more accurate approximations the previous references may be consulted. The inductance of a magnetic antenna is given by

$$L_a = n^2 \mu \frac{A_e}{l_e} \quad , \tag{2.15}$$

where n is the number of turns on the antenna.

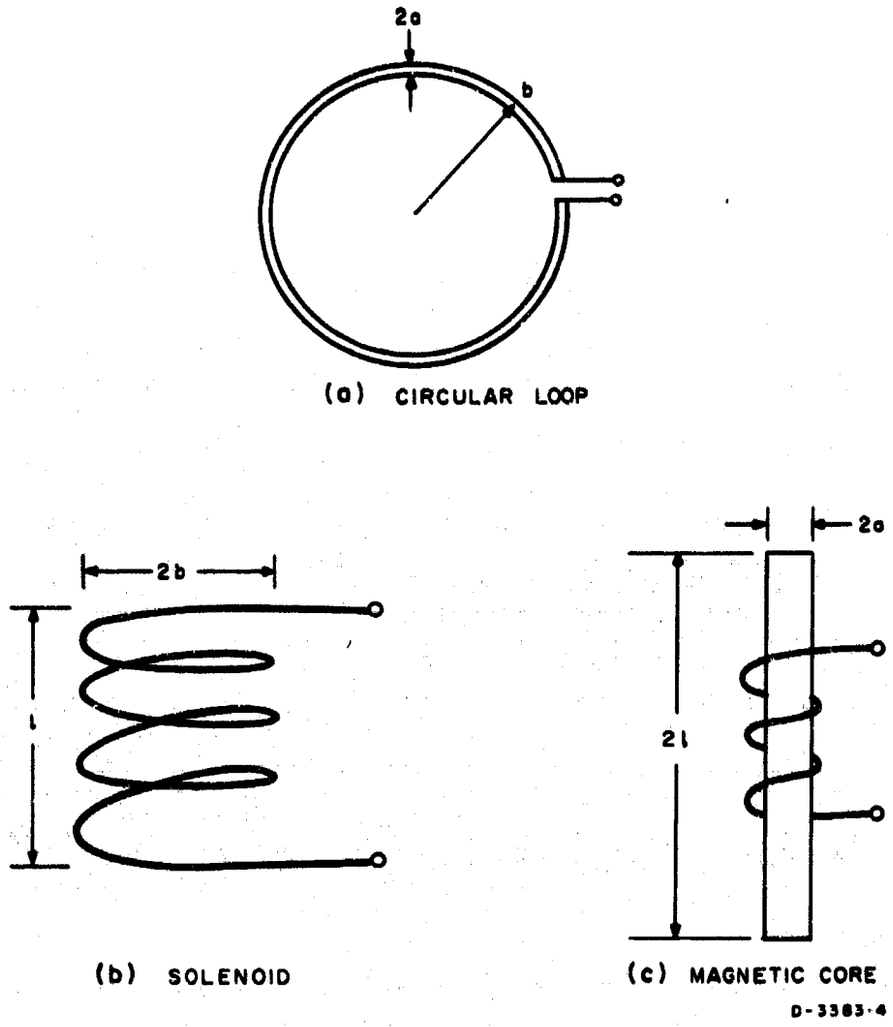

FIG. 2.2 INDUCTIVE ANTENNAS

In an antenna with a core of permeable magnetic material, such as that shown in Fig. 2.2(c), the effective area and volume will be a function of μ_i, the initial permeability of the core material. A good general approximation results from dividing the limiting effective area and effective volume shown in Table 2.1 by a factor β, where

$$\beta = 1 + \frac{2l^2\mu}{3a^2 \ln\left[\frac{l}{a} - 1\right]\mu_i} \quad . \tag{2.16}$$

In any case, the effective volume cannot exceed

$$\lim_{\mu_i a^2 \ll \mu l^2} \left(\frac{S}{\beta^2}\right) = \frac{3\pi a^2 l \mu_i}{2\mu}$$

$$= \frac{3\mu_i}{4\mu} \times \text{core volume} \quad , \tag{2.17}$$

which implies that the best use of a given amount of core material can be obtained by extending the length until this limit is approached.

A real capacitive antenna will have additional capacitance and probably loss associated with its feed point and transmission line or matching network, as shown in Fig. 2.3(a), where C_a is the antenna capacitance. This can be represented as the equivalent network shown, where

$$C_1 = C_a + C_b \tag{2.18}$$

$$l_1 = \frac{C_a l_e}{C_a + C_b} \tag{2.19}$$

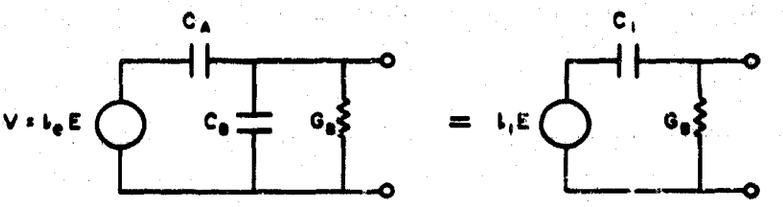

(a) CAPACITIVE

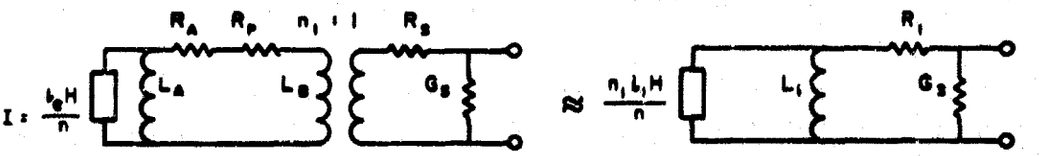

(b) INDUCTIVE

D-3383-3

FIG. 2.3 EQUIVALENT CIRCUITS OF ANTENNAS

$$S_1 = \frac{C_a S}{C_a + C_b} \tag{2.20}$$

are the equivalent capacitance, effective length, and effective volume. Another parameter which will be found useful later is the "intrinsic bandwidth,"

$$\Omega_a = \frac{G_b}{C_1} \quad . \tag{2.21}$$

The available power output from this real antenna is then

$$P_a = \frac{\omega^2 \epsilon E^2 S_1}{4\Omega_a} \quad . \tag{2.22}$$

A similar equivalence, shown in Fig. 2.3(b), can be established for inductive antennas which are transformer coupled. Here the antenna inductance is given by L_a, the antenna resistance R_a, the transformer primary inductance by L_b, the transformer primary resistance R_p, and the transformer secondary resistance by R_s. G_s is the conductance due to eddy-current losses. The parameters of the simplified equivalent are in general functions of frequency, but in the high-frequency limit they reduce to

$$L_1 = \frac{1}{n_1^2} \frac{L_a L_b}{L_a + L_b} \qquad \omega L_1 >> R_1 \tag{2.23}$$

$$R_1 = R_s + \frac{R_a + R_p}{n_1^2} \qquad \omega L_1 >> R_1 \tag{2.24}$$

$$l_1 = \frac{L_b l_e}{L_a + L_b} \qquad \omega L_1 >> R_1 \tag{2.25}$$

$$S_1 = \frac{L_b S}{L_a + L_b} \qquad \omega L_1 >> R_1 \quad . \tag{2.26}$$

The intrinsic bandwidth and available power are given by

$$\Omega_a = \frac{R_1}{L_1} + \omega^2 L_1 G_s \tag{2.27}$$

$$P_a = \frac{\omega^2 \mu H^2 S_1}{4\Omega_a} \quad . \tag{2.28}$$

Table 2.1

PROPERTIES OF SEVERAL TYPES OF SMALL ANTENNAS

	l_e	A_e	S	CONDITIONS
Capacitive	$\left\|\frac{V_0}{E}\right\|$	$\left\|\frac{I_s}{\omega D}\right\|$	$\left\|\frac{V_0 I_s}{\omega \epsilon E^2}\right\|$	
(a) Plate	d	ab	abd	$a \gg d$; $b \gg d$
(b) Flush plate	$\frac{\pi b}{4 ln(b/a)}$	πb^2	$\frac{\pi^2 b^3}{4 ln(b/a)}$	$d \gg b \gg a$
(c) Dipole	l	$\frac{\pi l^2}{ln(l/a) - 1}$	$\frac{\pi l^3}{ln(l/a) - 1}$	$l \gg a$
(d) Monopole	$\frac{l}{2}$	$\frac{\pi l^2}{ln(l/a) - 1}$	$\frac{(\pi/2) l^3}{ln(l/a) - 1}$	$l \gg a$
(e) Spheres	d	$\pi a d$	$\pi a d^2$	$d \gg a$
(f) T	d	$\frac{2\pi b d}{ln(2d/a)}$	$\frac{2\pi b d^2}{ln(2d/a)}$	$b \gg d \gg a$
Inductive	$\left\|\frac{n I_s}{H}\right\|$	$\left\|\frac{V_0}{n\omega B}\right\|$	$\left\|\frac{V_0 I_s}{\omega \mu H^2}\right\|$	
(a) Loop	$\frac{\pi b}{ln(b/a)}$	πb^2	$\frac{\pi^2 b^3}{ln(b/a)}$	$b \gg a$
(b) Solenoid	$l + 0.9b$	πb^2	$\pi b^2 (l + 0.9b)$	$l > 0.8b$
(c) Magnetic Core	l	$\frac{\pi l^2}{ln(l/a) - 1}$	$\frac{\pi l^3}{ln(l/a) - 1}$	$l \gg a$; $\mu_s a^2 \gg \mu_0 l^2$

BLANK PAGE

3. NOISE CHARACTERIZATION

It has been shown, by the IRE Subcommittee 7.9 on Noise [1960], for example, that any noisy, two-terminal pair network can be represented by an equivalent but noiseless network with a noise voltage generator and a noise current generator at its input such as that depicted in Fig. 3.1. In general, these noise generators will be partly correlated, which we can represent by letting

$$V_n = V_u + I_n Z_\gamma = V_u + I_n(R_\gamma + jX_\gamma) \quad , \tag{3.1}$$

where V_u and I_n are uncorrelated. For convenience, all noise sources used here are defined as rms values per hertz bandwidth. If the amplifier of Fig. 3.1 has a voltage gain A,

$$V_{out} = \frac{AZ_{in}}{Z_{in} + N^2 Z_t} [NV_t + V_u + I_n(Z_\gamma + N^2 Z_t)] \quad . \tag{3.2}$$

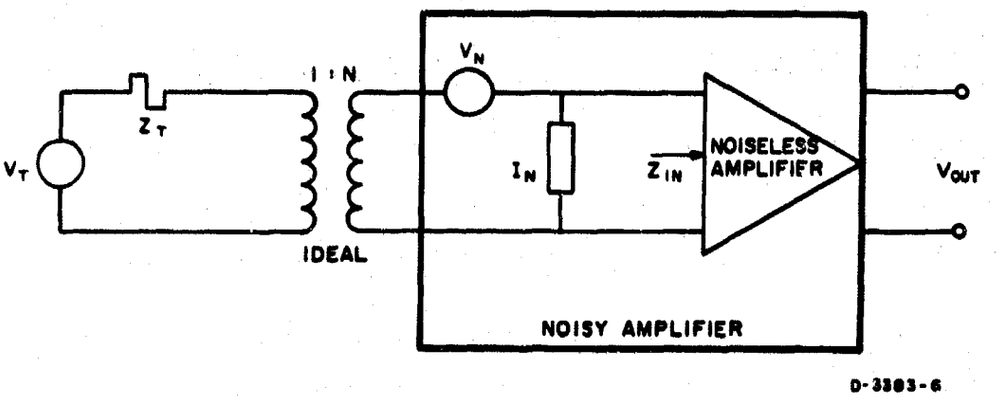

FIG. 3.1 EQUIVALENT CIRCUIT OF A NOISY AMPLIFIER

Then the ratio of available noise power to available signal power at the output is

$$\frac{P_n}{P_s} = \frac{\overline{V_u^2} + \overline{I_n^2}(Z_\gamma + N^2 Z_t)(Z_\gamma + N^2 Z_t)^*}{N^2 V_t^2}$$

$$= \frac{\overline{V_u^2} + \overline{I_n^2}[(R_\gamma + N^2 R_t)^2 + (X_\gamma + N^2 X_t)^2]}{N^2 V_t^2} \quad , \qquad (3.3)$$

where $\overline{\ }$ indicates time average, and * indicates complex conjugate. P_n/P_s has a minimum with respect to N when

$$N^4 = N_0^4 = \frac{\overline{V_u^2} + \overline{I_n^2}(R_\gamma^2 + X_\gamma^2)}{\overline{I_n^2}(R_t^2 + X_t^2)} = \frac{\overline{V_u^2} + \overline{I_n^2}|Z_\gamma|^2}{\overline{I_n^2}|Z_t|^2} \quad . \qquad (3.4)$$

The source impedance Z_s actually presented to the input terminals of the amplifier is then given by

$$|Z_{so}|^2 = N_0^4 |Z_t|^2 = \frac{\overline{V_n^2} + \overline{I_n^2}|Z_\gamma|^2}{\overline{I_n^2}} = \frac{\overline{V_n^2}}{\overline{I_n^2}} \quad . \qquad (3.5)$$

If R_s is independent of X_s, the minimum possible value of Eq. (3.3) is found for

$$Z_{so} = (\overline{V_u^2}/\overline{I_n^2} + R_\gamma^2)^{1/2} - jX_\gamma \quad , \qquad (3.6)$$

which is equivalent to providing a conjugate match for $Z_n = Z_{so}^*$. Since the signal power available from the source is

$$P_{as} = V_s^2/4R_s \quad , \qquad (3.7)$$

and the available noise power referred to the source is

$$P_{an} = P_{as}\frac{P_n}{P_s} \quad , \qquad (3.8)$$

the "noise temperature" of the amplifier can be defined by

$$KT_n \triangleq P_{an} = \frac{\overline{V_u^2} + \overline{I_n^2}|Z_\gamma + Z_s|^2}{4R_s} \quad , \tag{3.9}$$

where $K = 1.38 \times 10^{-23}$ J/°K, Boltzmann's constant. The minimum possible value of amplifier noise temperature is then

$$T_{no} = \frac{\overline{I_n^2}R_\gamma + (\overline{V_u^2}\,\overline{I_n^2} + \overline{I_n^4}R_\gamma^2)^{1/2}}{2K} \quad , \tag{3.10}$$

obtained when the source impedance has the value given by Eq. (3.6).

It is sometimes more convenient to express a noisy network in terms of admittances rather than impedances. The network could then be characterized by

$$I_n = I_u + V_n Y_\gamma = I_u + V_n(G_\gamma + jB_\gamma) \tag{3.11}$$

$$T_n = \frac{\overline{I_u^2} + \overline{V_n^2}|Y_\gamma + Y_s|^2}{4KG_s} \tag{3.12}$$

$$T_{no} = \frac{\overline{V_n^2}G_\gamma + (\overline{I_u^2}\,\overline{V_n^2} + \overline{V_n^4}R_\gamma)^{1/2}}{2K} \tag{3.13}$$

$$Y_{so} = (\overline{I_u^2}/\overline{V_n^2} + G_\gamma^2)^{1/2} - jB_\gamma \quad , \tag{3.14}$$

and transformations between the two descriptions can be made by

$$Y_\gamma = 1/Z_\gamma \tag{3.15}$$

$$\overline{I_u^2} = \overline{V_u^2}/|Z_\gamma|^2 \tag{3.16}$$

$$\overline{V_n^2} = \overline{V_u^2} + \overline{I_n^2}|Z_\gamma|^2 \tag{3.17}$$

$$\overline{V_u^2} = \overline{I_u^2}/|Y_\gamma|^2 \tag{3.18}$$

$$\overline{I_n^2} = \overline{I_u^2} + \overline{V_n^2}|Y_\gamma|^2 \quad . \tag{3.19}$$

For the purposes of improving stability, controlling frequency response, and simplifying alignment, it is frequently desirable to incorporate negative feedback in low-noise preamplifiers. This will usually result in reduced available gain G_a, because for an amplifier with voltage gain A, feedback factor β, and output impedance $Z_{out} = R_{out} + jX_{out}$,

$$A' = \frac{A}{1 - A\beta} \tag{3.20}$$

and

$$Z'_{out} = \frac{Z_{out}}{1 - A\beta} \tag{3.21}$$

are the gain and output impedance with feedback, as shown, for example, by Bode [1945]. The available gain is then

$$G_a = \frac{V_{out}^2 R_s}{V_s^2 R_{out}} = \frac{AR_s}{R_{out}(1 - A\beta)} \tag{3.22}$$

which is reduced by negative feedback (real part of $A\beta < 0$). Conversely, G_a may be increased by positive feedback at the expense of bandwidth and stability, but this is sometimes desirable if the second stage is noisy and the first stage gain is low.

Feedback can also be used to change the amplifier input impedance Z_{in} to Z'_{in}, which may be arbitrarily chosen from a wide range of values. The effect of this on noise characterization can be seen by referring to Fig. 3.2(a), an equivalent circuit of a noisy amplifier with both voltage and current feedback, represented by the Y-matrix networks Y_v and Y_i, respectively. The effect of these feedback networks on gain, terminal impedances, and noise can be readily determined by transforming this network into the equivalent shown in Fig. 3.3(b), where

$$I_i = Y_{i12} V_{out} + (4KT_1 G_{i22})^{1/2} \tag{3.23}$$

and

$$I_v = Y_{v12} V_{out} + (4KT_1 G_{v22})^{1/2} \tag{3.24}$$

where Y_{i12}, Y_{v12} are the transfer admittances and G_{i22}, G_{v22} the real parts of the self admittances at terminal 2 of the networks Y_i, Y_v respectively. T_1 is the temperature of the lossy elements in the networks. It is immediately apparent that the noise voltage and current

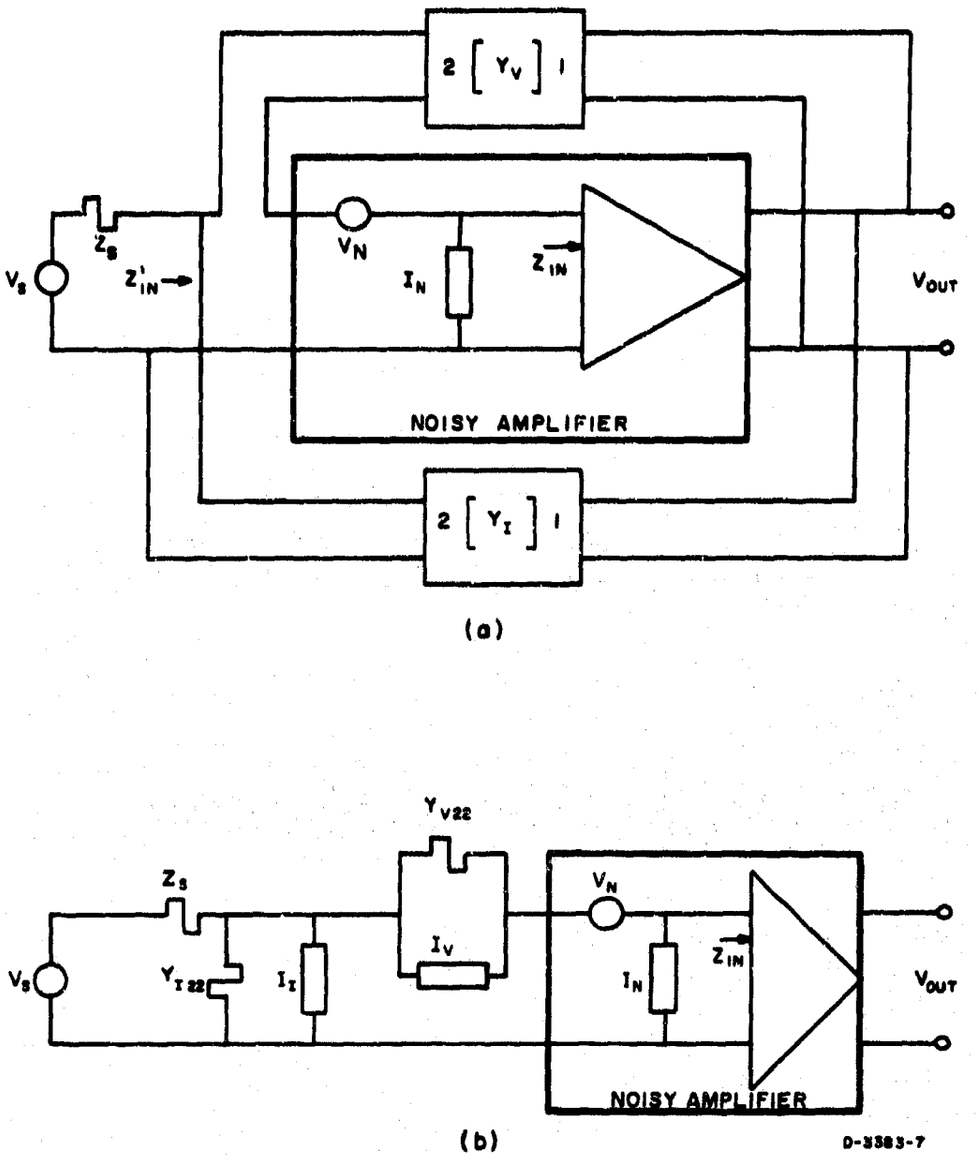

FIG. 3.2 NOISY AMPLIFIER WITH FEEDBACK

generators V_n and I_n which characterize the amplifier, assuming $V_n = V_u + I_n Z_\gamma$, can be replaced by new generators defined by

$$V'_n = V'_u + I_n Z_\gamma \qquad (3.25)$$

$$\overline{V_u'^2} = \overline{V_u^2} + \frac{4KT_1G_{v22}}{y_{v22}y_{v22}^*} \tag{3.26}$$

$$\overline{I_n'^2} = \overline{I_n^2} + KT_1G_{i22} \tag{3.27}$$

The equivalent feedback generators then become

$$I_i' = Y_{i12}V_{out} \tag{3.28}$$

$$I_v' = Y_{v12}V_{out} \tag{3.29}$$

and the resulting network can be analyzed by the usual feedback amplifier methods, with the result that the available gain, but not the equivalent noise generators, may be further modified by the feedback. The total effect is therefore that of adding to the source the physical elements introduced by the feedback networks (which will modify the amplifier gain because of source transformation, and may increase the apparent amplifier noise) and modifying the available gain by feedback.

Having included the above feedback effects in the amplifier noise characterization, the performance of a complete system can be calculated by including the thermal noise due to the real part R_s of the source impedance Z_s, still referring to Fig. 3.2. Assuming that the source network is at the temperature T_r, this noise appears as a voltage V_r in series with Z_s, and is given by

$$\overline{V_r^2} = 4KT_rR_s \quad . \tag{3.30}$$

The output noise-to-signal ratio is then

$$\frac{P_n}{P_s} = \frac{\overline{V_u^2} + \overline{I_n^2}|Z_\gamma + Z_s|^2 + 4KT_rR_s}{V_s^2} \quad . \tag{3.31}$$

By an approach similar to Eqs. (3.3) to (3.9), the system noise temperature can be defined as

$$T_s \doteq \frac{P_{as}P_n}{KP_s} = \frac{\overline{V_u^2} + \overline{I_n^2}|Z_\gamma + Z_s|^2 + 4KT_rR_s}{4KR_s} = T_r + T_n \tag{3.32}$$

and the signal-to-noise (per unit bandwidth) ratio is

$$\frac{P_s}{P_n} = \frac{V_s^2}{4KT_sR_s} \quad . \tag{3.33}$$

If noisy amplifiers A_1, A_2, A_3, ... with respective available power gains (in the system) G_{a1}, G_{a2}, G_{a3}, ... and respective noise temperatures (in the system) T_{n1}, T_{n2}, T_{n3}, ... are cascaded, the resultant noise-to-signal ratio is

$$\frac{P_n}{P_s} = \frac{K(T_r + T_{n1})G_{a1}G_{a2}G_{a3} \ \ldots \ + KT_{n2}G_{a2}G_{a3} \ \ldots \ + KT_{n3}G_{a3} \ \ldots \ + \ \ldots}{P_{as}G_{a1}G_{a2}G_{a3} \ \ldots} \tag{3.34}$$

and the system noise temperature becomes

$$T_s = T_r + T_{n1} + \frac{T_{n2}}{G_{a1}} + \frac{T_{n3}}{G_{a1}G_{a2}} + \ \ldots \tag{3.35}$$

Minimizing this T_s is equivalent to placing the available amplifiers in the order of increasing "noise measure" M [Haus and Adler, 1959] with

$$M_i = \frac{F_i - 1}{1 - \frac{1}{G_{ai}}} = \frac{T_{ni}}{T_a\left(1 - \frac{1}{G_{ai}}\right)} \tag{3.36}$$

for the ith amplifier, where $F_i = 1 + (T_{ni}/T_a)$ is the familiar "noise figure," T_a is a reference temperature (usually 293°K), and G_{ai} is the available power gain.

If the output of the noisy amplifier is subsequently filtered by a network with transfer function $J(\omega)$, the signal-to-noise ratio at the output will be

$$\frac{P_s(\omega_1)}{P_{nt}} = \frac{2\pi P_{as}(\omega_1)J(\omega_1)J^*(\omega_1)}{K\int_0^\infty T_a(\omega)J(\omega)J^*(\omega)\,d\omega} \tag{3.37}$$

where the signal is at angular frequency ω_1, and P_{nt} is the total rms noise.

BLANK PAGE

4. NOISE IN AMPLIFYING DEVICES

In this section the noise characterization, as developed in Sec. 3, will be derived for three types of amplifiers: bipolar junction transistors, junction-gate unipolar field-effect transistors, and a double-sideband semiconductor diode parametric amplifier. Other devices available at this time do not appear to offer significant sensitivity advantage over the above three. For instance, metal-oxide semiconductor (MOS) or "insulated gate" field-effect transistors behave very much like junction-gate transistors except for three significant points: First, the equivalent noise voltage is considerably larger than in a junction-gate device of similar input capacity. Second, the equivalent noise current at low frequencies is very much lower than in a junction-gate device, and is proportional to frequency rather than flat, as shown by Jordan and Jordan [1965]. Third, flicker noise (also discussed by Jordan and Jordan) is a predominant effect to much higher frequencies (10-100 kHz) than in junction-gate devices, where it is usually important only below 1 to 10 kHz. In all three respects, the MOS transistor is remarkably similar to a vacuum tube, and in both cases the disadvantages of the first and last points outweigh the advantage of the second point for virtually all practical applications, since the extremely high source resistance required cannot be obtained. Therefore, they will not be considered further at this time.

In the development of noise performance which follows, flicker noise will be ignored since it is very strongly dependent on the particular device involved. Suffice to say that parametric amplifiers are by far the best in this respect; flicker noise being unobservable in one case [Biard, 1963] at frequencies down to 1 Hz. Bipolar junction transistors are intermediate, with flicker noise cutoffs generally in the range of 100 to 1000 Hz.

One type of amplifier that is extremely promising has not been considered here because it has not yet been thoroughly investigated. This is a double-sideband inductive parametric amplifier, which should be ideally suited for use with inductive antennas. Once its noise sources

are understood, it should be easy to analyze such a device as the dual of the capacitive amplifier considered here. While ordinary saturating ferrite elements could be used as the time-varying inductance in a parametric amplifier, these devices are known to be noisy. However, the work of Deaver and Goree [1965] has led to a superconducting magnetic modulator which is capable of the necessary switching speed and should prove to have extremely low noise.

4.1 BIPOLAR JUNCTION TRANSISTORS

The physical sources of noise in junction transistors are thoroughly discussed by van der Ziel [1958], and his results will be adopted without further discussion. Referring to the equivalent circuit of Fig. 4.1, the signal source is a voltage V_s and impedance $Z_s = R_s + jX_s$, all functions of angular frequency ω. Except for notation, the internal noise sources V_b, I_1, and I_2 are those of van der Ziel's model, as are the base spreading resistance $r_{bb'}$, the emitter junction admittance $Y_e = G_e + jB_e$, and the collector junction admittance Y_c. Assuming the transistor is used in the common-emitter connection, which usually has the lowest noise measure because of its high available gain, and letting $Y_c = 0$ since we are not interested in extremely high frequencies, the short circuit collector output current is found to be

$$I_c = \frac{\alpha(V_s + V_b) + \alpha I_1(Z_s + r_{bb'}) + I_2(Z_s + r_{bb'} + Z_e)}{(Z_s + r_{bb'})(1 - \alpha) + Z_e} \qquad (4.1)$$

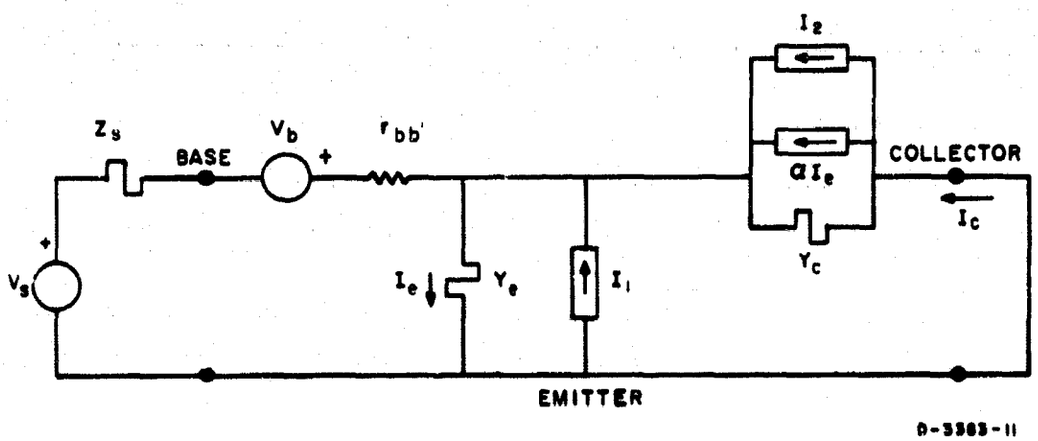

FIG. 4.1 NOISY JUNCTION TRANSISTOR

where α is the collector-to-emitter forward current transfer function and $Z_e = 1/Y_e$. Letting $I_c = 0$, the value of V_s can be found which would exactly cancel the internal noise sources

$$-V_s(I_c = 0) = V_n + I_n Z_s = V_b + I_1(Z_s + r_{bb'}) + \frac{I_2(Z_s + r_{bb'} + Z_e)}{\alpha} \tag{4.2}$$

and V_n and I_n are the desired equivalent noise sources referred to the input, as in Sec. 3. Collecting coefficients of Z_s,

$$V_n = V_b + I_1 r_{bb'} + I_2 \frac{r_{bb'} + Z_e}{\alpha} \tag{4.3}$$

$$I_n = I_1 + \frac{I_2}{\alpha} \tag{4.4}$$

But the noise sources, as derived by van der Ziel, are

$$\overline{V_b^2} = 4KTr_{bb'} \tag{4.5}$$

$$\overline{I_1^2} = 4KTG_e - 2qI_e \tag{4.6}$$

$$\overline{I_2^2} = 2qI_c \tag{4.7}$$

$$\overline{I_1^* I_2} = 2KTY_{ce} \tag{4.8}$$

where K is Boltzmann's constant, T is the transistor temperature, q is the charge of an electron, I_e is the dc emitter current, I_c is the dc collector current, and Y_{ce} is the collector-to-emitter transadmittance. Adopting the approximations of Nielson [1957], which have been shown to be valid for frequencies well below the α cutoff frequency f_α, results in

$$r_e = \frac{1}{G_e} = \frac{KT}{qI_e} \tag{4.9}$$

$$Y_{ce} = \frac{\alpha}{r_e} \tag{4.10}$$

$$\overline{I_1^2} = \frac{2KT}{r_e} \tag{4.11}$$

$$I_2 = -\alpha I_1 + I_3 \tag{4.12}$$

$$\overline{I_3^2} = \frac{2KT}{r_e}(\alpha_0 - |\alpha|^2) \tag{4.13}$$

where r_e is the emitter junction resistance, I_3 is the component of I_2 that is uncorrelated with I_1, and α_0 is the dc α. Letting $V_n = V_n + I_n Z_\gamma$, and approximating α with

$$\alpha = \frac{\alpha_0}{1 + j\Omega_\alpha} \tag{4.14}$$

where $\Omega_\alpha = f/f_\alpha$, the noise characterization is

$$\overline{I_n^2} = \frac{2KT(1 - \alpha_0 + \Omega_\alpha^2)}{r_e(1 + \Omega_\alpha^2)^{1/2}} \tag{4.15}$$

$$\overline{V_u^2} = 2KT(r_e + 2r_{bb'}) \tag{4.16}$$

$$Z_\gamma = R_\gamma = r_e + r_{bb'} \tag{4.17}$$

which result in

$$T_n = \frac{T}{2R_s}\left\{r_e + 2r_{bb'} + \frac{(1 - \alpha_0 + \Omega_\alpha^2)[(R_s + r_e + r_{bb'})^2 + X_s^2]}{(1 + \Omega_\alpha^2)^{1/2} r_e}\right\} \tag{4.18}$$

$$Z_{so} = R_{so} = \left[\frac{r_e(r_e + 2r_{bb'})(1 + \Omega_\alpha^2)^{1/2}}{1 - \alpha_0 + \Omega_\alpha^2} + (r_e + r_{bb'})^2\right]^{1/2} \tag{4.19}$$

Typical values of these parameters for germanium and silicon transistors selected for low noise at low frequencies are given in Table 4.1.

4.2 FIELD-EFFECT TRANSISTORS

The noise model of a field-effect transistor developed by van der Ziel [1962], and supported by the measurements of Bruncke [1963], leads to an equivalent circuit similar to Fig. 4.2. In this circuit, the signal source is a current I_a and admittance Y_a connected between the transistor source

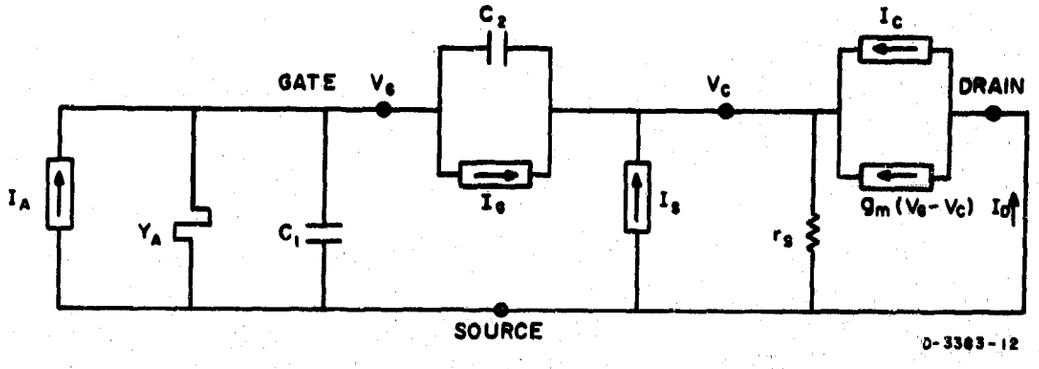

FIG. 4.2 NOISY FIELD-EFFECT TRANSISTOR

and gate. C_2 is the capacitance between the gate and the active channel of the device, and C_1 is the rest of the input capacitance, including strays. The resistance r_s is the ohmic resistance between the source terminal and the channel, which is the node labeled V_c; and g_m is the actual transconductance referred to the voltage between gate and channel. I_g, I_s, and I_c are noise currents evaluated below. Proceeding as in Sec. 4.1, the short-circuit drain current is zero if

$$I_a = I_g(1 + Y_a r_s + j\omega C_1 r_s) + I_s r_s (Y_a + j\omega C_1)$$

$$- \frac{I_c}{g_m} [(Y_a + j\omega C_1)(1 + j\omega C_2 r_s) + j\omega C_2] \quad . \qquad (4.20)$$

Collecting coefficients of Y_a and reversing all signs, which is equivalent to reversing the phases of the noise generators,

$$V_n = I_g r_s + I_s r_s - I_c \frac{1 + j\omega C_2 r_s}{g_m} \qquad (4.21)$$

$$I_n = I_g(1 + j\omega C_1 r_s) + I_s j\omega C_1 r_s + I_c \frac{\omega^2 C_1 C_2 r_s - j\omega(C_1 + C_2)}{g_m} \quad . \tag{4.22}$$

Letting $I_n = I_u + Y_\gamma V_n$, we find that an array of admittances is necessary to specify Y_γ, since the noise currents have different coefficient ratios. Labeling Y_γ components with the subscripts of the corresponding noise currents,

$$I_u = 0 \tag{4.23}$$

$$Y_{\gamma g} = \frac{1}{r_s} + j\omega C_1 \tag{4.24}$$

$$Y_{\gamma s} = j\omega C_1 \tag{4.25}$$

$$Y_{\gamma c} = \frac{j\omega(C_1 + C_2) - \omega^2 C_1 C_2 r_s}{1 + j\omega C_2 r_s} \tag{4.26}$$

The noise current magnitudes are given by

$$\overline{I_g^2} = 2qI_{g0} \tag{4.27}$$

$$\overline{I_s^2} = \frac{4KT}{r_s} \tag{4.28}$$

$$\overline{I_c^2} = 4KTQg_m \tag{4.29}$$

where I_{g0} is the sum of the magnitudes of all electron and hole currents to and from the gate. I_{g0} approaches the gate cutoff current for reverse bias. Q is the space-charge smoothing factor, generally lying between 0.6 and 0.67. In any practical device, $I_s^2 >> I_g^2$, and the I_g term can be dropped from Eq. (4.21). For the low-frequency case, $\omega C_1 r_s << 1$, and $\omega C_2 r_s << 1$, and

$$V_n = I_s r_s - \frac{I_c}{g_m} \tag{4.30}$$

$$\overline{V_n^2} = 4KT\left(r_s + \frac{Q}{g_m}\right) \approx KT\left(4r_s + \frac{2.5}{g_m}\right) \tag{4.31}$$

$$\overline{I_u^2} = 2qI_{g0} \tag{4.32}$$

$$Y_{\gamma s} = j\omega C_1 \tag{4.33}$$

$$Y_{\gamma c} = j\omega(C_1 + C_2) \tag{4.34}$$

Since C_2 is generally less than half as large as C_1, particularly if C_1 includes external strays,

$$Y_\gamma = j\omega C_1 \tag{4.35}$$

and

$$T_n = \frac{2qI_{g0} + KT\left(4r_s + \frac{2.5}{g_m}\right)\left[G_s^2 + (B_s + \omega C_1)^2\right]}{4KG_s} \tag{4.36}$$

$$Y_{so} = \left[\frac{2qI_{g0}}{KT\left(4r_s + \frac{2.5}{g_m}\right)}\right]^{1/2} - j\omega C_1 \tag{4.37}$$

Typical values of noise parameters are given in Table 4.1. It must be remembered, however, that the low noise temperature indicated cannot be realized at frequencies below 1 to 10 kHz because of flicker noise, which generally raises not only the minimum noise temperature T_{no} but also R_{so}.

4.3 A PARAMETRIC AMPLIFIER

Realization of power gain by the use of a periodically time-varying reactance, generally called "parametric amplification," is a well-known technique at UHF and microwave frequencies. This subject has been well developed (see, for example, Blackwell and Kotzebue [1961] mainly because of the extremely good noise performance obtainable. Some of the same techniques could be applied at low frequencies, but they would be limited to fixed-tuned narrowband systems. As will be seen in Sec. 5, there is very little to be gained over a simple junction transistor in this case.

Sensitivity can, however, be significantly improved by lowering the amplifier noise temperature in a "broadband" application; that is, one in which sensitivity is important in a bandwidth very much wider than the "intrinsic bandwidth" of the antenna system Ω_a as defined in Sec. 2.

One type of parametric amplifier capable of this wideband operation is the double-sideband capacitive converter using semiconductor diodes, such as that described by Biard [1963]. This device can be analyzed by considering the equivalent circuit of Fig. 4.3. In this circuit the signal source is the current I_a, at angular frequency ω_1, and the admittance Y_a, where Y_a is assumed to include elements which provide a short circuit in the vicinity of the pump frequency as described below. The nonlinear capacitors being "pumped" at frequency ω_3 are represented by the admittance matrix $[Y_v]$, as described by Blackwell and Kotzebue. $Y_b = G_b + jB_b$ is the admittance at the output terminals of the converter, and the output voltage V_b consists of the two sidebands V_{b2} and V_{b4} at frequencies $\omega_2 = \omega_3 - \omega_1$ and $\omega_4 = \omega_3 + \omega_1$, respectively. In operation, V_b is coherently detected with respect to a pump signal of the appropriate phase, or envelope detected with a superimposed carrier, to recover the amplified original signal. The noise sources are I'_v, which include the diode shot noise and thermal resistance noise of the series combination of diodes, transformers and inductors; and I_b, the additional noise added by Y_b, the load admittance. Since we have shown in Sec. 3 that the input noise current of an amplifier does not have to be related to its input impedance, and G_b can be provided by feedback from a following amplifier, we will not assume that I_b is the thermal conductance noise of G_b, as Biard has done.

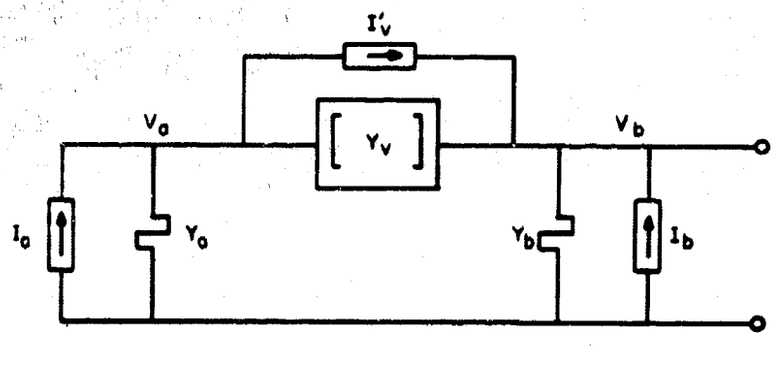

FIG. 4.3 NOISY DOUBLE-SIDEBAND PARAMETRIC AMPLIFIER

Denoting the current or voltage at frequency ω_i as I_i or V_i, and expressing the time-varying capacitance as

$$C(t) = C_0[1 + 2\gamma_1 \cos \omega_3 t + 2\gamma_2 \cos 2\omega_3 t] \quad , \tag{4.38}$$

the current through the element labeled $[Y_v]$ is related to the voltage across it by

$$\begin{bmatrix} I^*_{c2} \\ I_{c1} \\ I_{c4} \end{bmatrix} = jC_0 \begin{bmatrix} -\omega_2 & -\omega_2\gamma_1 & -\omega_2\gamma_2 \\ \omega_1\gamma_1 & \omega_1 & \omega_1\gamma_1 \\ \omega_4\gamma_2 & \omega_4\gamma_1 & \omega_4 \end{bmatrix} \begin{bmatrix} V^*_{c2} \\ V_{c1} \\ V_{c4} \end{bmatrix} \tag{4.39}$$

Subscripting components of the voltages and currents of Fig. 4.3 according to frequency and letting Y_a be infinite at ω_2 and ω_4 ($V_{a2} = V_{a4} = 0$), and letting Y_b be infinite at ω_1 ($V_{b1} = 0$), we can write three independent equations for the sums of current components at nodes A and B;

$$0 = I_{a1} - I'_{v1} - V_{a1}(Y_c + j\omega_1 C_0) + j\omega_1 C_0\gamma_1 V^*_{b2} + j\omega_1 C_0\gamma_1 V_{b4} \tag{4.40}$$

$$0 = I^*_{b2} + I'^*_{v2} - Y^*_b V^*_{b2} + j\omega_2 C_0(V^*_{b2} - \gamma_1 V_{a1} + \gamma_2 V_{b4}) \tag{4.41}$$

$$0 = I_{b4} + I'_{v4} - Y_b V_{b4} - j\omega_4 C_0(\gamma_2 V^*_{b2} - \gamma_1 V_{a1} + V_{b4}) \quad . \tag{4.42}$$

For pump-frequency resonance at node B, letting

$$Y_b = G_b + \frac{1}{j\omega L} \tag{4.43}$$

results in

$$\omega_3^2 LC_0 = 1 \tag{4.44}$$

$$Y_b(\omega_2) = G_b - j\frac{p_0^2}{d_0} \tag{4.45}$$

$$Y_b(\omega_4) = G_b - j\frac{p_0^2}{s_0} \tag{4.46}$$

where

$$p_0 = \omega_3 C_0$$

$$d_0 = \omega_2 C_0$$

$$s_0 = \omega_4 C_0$$

and Eqs. (4.40) through (4.42) can be written in matrix form

$$\begin{bmatrix} I_1 \\ I_2^* \\ I_4 \end{bmatrix} = \begin{bmatrix} Y_a + ja_0 & -ja_1 & -ja_1 \\ jd_1 & G_b + ja_{02} & -jd_2 \\ -js_1 & js_2 & G_b + ja_{04} \end{bmatrix} \begin{bmatrix} V_{a1} \\ V_{b2}^* \\ V_{b4} \end{bmatrix} \tag{4.47}$$

where

$$I_1 = I_{a1} - I'_{v1}$$

$$I_2 = I_{b2}^* + I'^*_{v2}$$

$$I_4 = + I'_{v4}$$

$$a_0 = \omega_1 C_0 \qquad a_1 = \omega_1 C_0 \gamma_1$$

$$d_1 = \omega_2 C_0 \gamma_1 \qquad d_2 = \omega_2 C_0 \gamma_2$$

$$s_1 = \omega_4 C_0 \gamma_1 \qquad s_2 = \omega_4 C_0 \gamma_2$$

$$a_{02} = a_0 \left(1 + \frac{a_0}{2d_0}\right)$$

$$a_{04} = a_0 \left(1 - \frac{a_0}{2s_0}\right) .$$

Solving for V_{b2}^* and V_{b4},

$$V_{b2}^* D = I_1[a_{04}d_1 - s_1 d_2 - jd_1 G_b] + I_2^*[(Y_a + ja_0)(G_b + ja_{04}) + a_1 s_1]$$

$$+ I_4[a_1 d_1 - a_0 d_2 + jd_2 Y_a] \tag{4.48}$$

$$V_{b4}D = I_1[-d_1 s_2 - a_{02} s_1 + j s_1 G_b] + I_2^*[a_0 s_2 - a_1 s_1 - j s_2 Y_a]$$

$$* I_4[(Y_a + j a_0)(G_b + j a_{02}) - a_1 d_1] \qquad (4.49)$$

and

$$D = (Y_a + j a_0)[(G_b + j a_{02})(G_b + j a_{04}) - d_2 s_2]$$

$$+ a_1 s_1 (G_b + j a_{02} + j d_2) - a_1 d_1 (G_b + j a_{04} - j s_2) . \qquad (4.50)$$

The process of optimum detection amounts to multiplying V_b by a pump-frequency carrier at one of the two phases which result in the signal components of V_{b2} and V_{b4} appearing in phase, followed by low-pass filtering. This is equivalent, in our notation, to cross-multiplying Eqs. (4.48) and (4.49) by unit phasors, each having the phase angle of the I_1 coefficient of the opposite equation, and adding. Performing this operation and letting $\omega_4 - \omega_3 - 0 = \omega_3 - \omega_2$, since $\omega_3 >> \omega_1$, we can set the detected voltage to zero and solve for I_1:

$$2p_1 I_1 = I_2\left[jY_a - a_0 + \frac{2G_b(j a_1 p_1 - j a_0 p_2 - p_2 Y_a)}{p_2^2 + G_b^2}\right]$$

$$+ I_3\left[\frac{(p_2^2 - G_b^2)(a_0 - jY_a) - 2a_1 p_1 p_2}{p_2^2 + G_b^2}\right] \qquad (4.51)$$

where

$$p_1 = \omega_3 C_0 \gamma_1$$

$$p_2 = \omega_3 C_0 \gamma_2 .$$

If the noise current I_v' consists of a true current I_v across $[Y_v]$ and a current equivalent due to the effect of an uncorrelated noise voltage V_v in series with $[Y_v]$, the ω_1 component of I_v' is

$$I_{v1}' = I_v + V_v(Y_a + j a_0) \qquad (4.52)$$

which results in an equivalent source noise current and voltage

$$I_n = I_v + j a_0 V_v + I_2\left[\frac{-a_0(G_b^2 + p_2^2) + 2jG_b(a_1 p_1 - a_0 p_2)}{2p_1(G_b^2 + p_2^2)}\right] + I_4\left[\frac{-a_0(G_b^2 - p_2^2) - 2a_1 p_1 p_2}{2p_1(G_b^2 + p_2^2)}\right] \qquad (4.53)$$

$$V_n = V_v + I_2 \left[\frac{j(G_b^2 + p_2^2) - 2G_b p_2}{2p_1(G_b^2 + p_2^2)}\right] + I_4 \left[\frac{j(G_b^2 - p_2^2)}{2p_1(G_b^2 + p_2^2)}\right] \tag{4.54}$$

Lumping all resistive noise sources in $[Y_v]$ and Y_b into I_b, including the high-frequency components of V_v,

$$\overline{I_2^2} = \overline{I_4^2} = \overline{I_b^2} + \overline{I_v'^2} \tag{4.55}$$

and letting

$$I_n = I_u + V_n Y_\gamma$$

$$\overline{V_n^2} = \overline{V_v^2} + \frac{\overline{I_b^2} + \overline{I_v^2}}{2p_1^2} \tag{4.56}$$

$$\overline{I_u^2} = \overline{I_v^2} \tag{4.57}$$

$$Y_{\gamma v} = ja_0 \tag{4.58}$$

$$Y_{\gamma 2} = ja_0 + \frac{2a_1 p_1 G_b (G_b^2 + p_2^2) - 4ja_1 p_1 p_2 G_b^2}{G_b^4 + p_2^4 + 6G_b^2 p_2^2} \tag{4.59}$$

$$Y_{\gamma 4} = ja_0 + \frac{ja_1 p_1 p_2}{G_b^2 - p_2^2} \tag{4.60}$$

where $Y_{\gamma v}$ applies to the V_v component in Eq. (4.54), $Y_{\gamma 2}$ applies to the I_2 component, and $Y_{\gamma 4}$ applies to the I_4 component. Observing from Eq. (3.13) that T_{n0} will be minimized by minimizing G_γ, we wish to minimize the real part of Eq. (4.59). Since G_b is the only arbitrary parameter at our disposal, this can be done only by letting G_b become infinite. Assuming that the noise current I_v is due to the diode cutoff current I_{c0}; the noise voltage V_v is due to resistance R_v as discussed previously, and the noise current I_b is the sum of currents due to the real loss conductance G_1 reflected to Y_b and the uncorrelated current I_x from the following amplifier, the noise characterization becomes

$$\overline{V_n^2} = \overline{V_v^2} + \frac{\overline{I_b^2} + \overline{I_v^2}}{2p_1^2} = 4KTR_v + \frac{4KTG_1 + \overline{I_x^2} + 2qI_{c0}}{2\omega_3^2 C_0^2 \gamma_1^2} \tag{4.61}$$

$$I_u^2 = 2qI_{c0} \tag{4.62}$$

$$Y_\gamma = j\omega_1 C_0 \quad . \tag{4.63}$$

Table 4.1 includes predicted values of noise parameters calculated from the assumptions above for typical values of component characteristics, although this performance has not been completely experimentally verified. It should be pointed out here that the choice of making G_b infinite, while it minimizes noise temperature, may not always minimize noise measure, because available gain is reduced. At the same time, this choice maximizes amplifier bandwidth and stability, and may be used for these reasons. Although the performance of this type of amplifier appears very similar to that of a field-effect transistor, the obvious advantages of the parametric amplifier are in the designer's ability to choose diodes from a wide range of capacities to make Y_γ match a given source, and the virtual absence of flicker noise obtainable.

Table 4.1

TYPICAL NOISE CHARACTERISTICS OF AMPLIFIERS

PARAMETERS	SILICON TRANSISTOR	GERMANIUM TRANSISTOR	FET	PARAMP	UNIT
1. $\overline{v_u^2}$, $\left(\overline{v_n^2}\right)$	3×10^{-17}	6×10^{-18}	(10^{-16})	(10^{-19})	$\frac{v^2}{Hz}$
2. $\overline{I_n^2}$, $\left(\overline{I_u^2}\right)$	7×10^{-26}	4×10^{-25}	(10^{-28})	(10^{-27})	$\frac{a^2}{Hz}$
3. R_γ, (G_γ)	3,000	400	(0)	(0)	Ω, (℧)
4. $\frac{X_\gamma}{\omega}$, $\left(\frac{B_\gamma}{\omega}\right)$	(8)	(20)	(5)	(100)	(pf)
5. R_{so}, (G_{so})	20 K	4 K	(10^{-6})	(10^{-4})	Ω, (℧)
6. T_{no}	65	55	4	0.4	°K
7. $\frac{\Omega_p}{2\pi}$	10^6	2×10^6	3×10^4	1.5×10^5	Hz

Explanations:

1-5: Perentheses indicate admittance characterization.

4-5: The optimum source is $Z_{so} = R_{so} - jX_\gamma$

or

$$Y_{so} = G_{so} - jB_\gamma$$

6: Device noise temperature T_n when $Z_s = Z_{so}$

or

$$Y_s = Y_{so}$$

7: Intrinsic bandwidth $\Omega_p = \frac{R_{so}}{X_\gamma}$ or $\frac{G_{so}}{B_\gamma}$.

5. RECEIVING SYSTEM SENSITIVITY

In the previous sections, the characteristics of the essential parts of a sensitive VLF receiving system, namely the antenna and the preamplifier, have been investigated. It remains to put them together to see what can be said about the capabilities of a complete system. The critical problem is, of course, that of transforming the inherently reactive source as nearly as possible into the optimum for a particular amplifier. This is called "noise matching" and has been shown in Sec. 3 to be equivalent to inserting a lossless network between source and preamplifier which would transform the source to conjugate-match the impedance

$$\begin{aligned} Z_n &= Z_{so}^* \\ &= R_{so} - jX_{so} \\ &= R_{so} + jX_{so} \end{aligned} \tag{5.1}$$

This problem can be split into two parts, each of which is an example of the problem of matching a complex source impedance to a resistive load for maximum power transfer over the widest possible frequency range. A special case, that of a parallel conductance, capacitance, and current for the source, was first treated by Bode [1945]; the general solution was demonstrated by Fano [1950].

Following Fano's approach, we can represent our problem as in Fig. 5.1(a) by two sets of lossless networks, (N_1N_2) and (N_3N_4), terminated at each end by unit resistance. If the antenna terminal impedance is Z_a, let N_1 be a network such that the impedance Z_2 looking into N_1 is

$$Z_2 = Z_a = R_a + jX_a \quad . \tag{5.2}$$

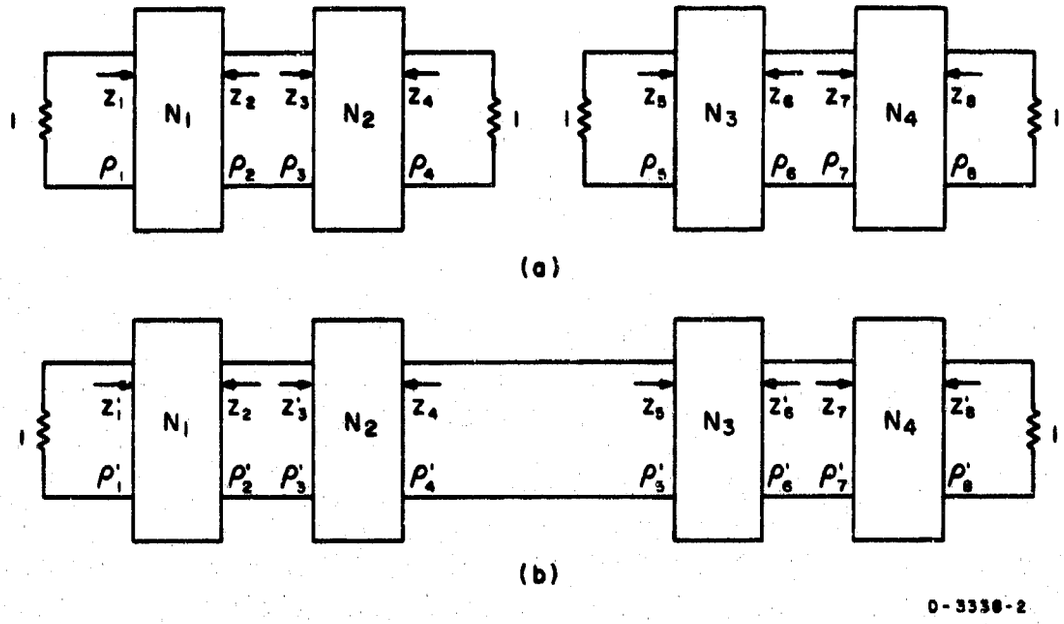

FIG. 5.1 NETWORKS FOR MATCHING ARBITRARY TERMINATION IMPEDANCES

If the impedance looking into N_2 from the same point is Z_3 as shown, the corresponding reflection coefficients are

$$\rho_2 = \frac{Z_2 - Z_3^*}{Z_2 + Z_3} \tag{5.3}$$

$$\rho_3 = \frac{Z_3 - Z_2^*}{Z_2 + Z_3} \tag{5.4}$$

for which it is clear that $|\rho_2| = |\rho_3|$. In fact, the magnitudes of all reflection coefficients in a chain of lossless networks must be equal. Now, Fano has shown that a lossless network N_2 can be realized which will present a reflection coefficient ρ_4 to a unit resistance as shown, provided

$$\int_0^\infty \ln\left|\frac{1}{\rho_4}\right| d\omega \leq \pi\lambda_0 \tag{5.5}$$

where

$$\Omega_a = \frac{1}{L_1} \qquad \text{(normalized)}$$

$$= \frac{R_a}{L_a} \tag{5.6}$$

in the general case if the first element at terminal 1 of N_1 is a series inductor L_1 for the normalized termination or L_a if the termination is R_a. Similarly, if the first element is a shunt capacitance C_1 (normalized)

$$\Omega_a = \frac{1}{C_1}$$

$$= \frac{G_a}{C_a} \tag{5.7}$$

in the general case. The intrinsic bandwidth Ω_a is thus the same parameter called Ω_a for the antennas described in Sec. 2. Most other cases of interest can be converted to one of the above by the general lowpass-to-bandpass transformation. Obviously, if Ω_a is finite, ρ_4 must approach unity except in some finite bandwidth ω_c called the passband.

Having determined a bound on bandwidth as a function of reflection coefficient, we next investigate the relation between sensitivity and reflection coefficient. If N_4 of Fig. 5.1(a) is a lossless network such that

$$Z_7 = Z_n = R_{so} + jX_\gamma \tag{5.8}$$

where Z_n is the "noise load" of Eq. (5.1), and $Z_6 = R_6 + jX_6$, we find

$$\rho_7 = \frac{Z_n - Z_6^*}{Z_n + Z_6} \quad . \tag{5.9}$$

Solving for Z_6,

$$Z_6 = R_{so}\frac{1 - \rho_7}{1 + \rho_7} - jX_\gamma \tag{5.10}$$

and from Eq. (3.9),

$$T_n = \frac{\overline{V_u^2} + \overline{I_n^2}\left|R_{so}\dfrac{1-\rho_7}{1+\rho_7} + R_\gamma\right|^2}{4K\ \mathrm{Re}\left(R_{so}\dfrac{1-\rho_7}{1+\rho_7}\right)} \tag{5.11}$$

where Re denotes "the real part of". Noting from Eq. (3.6) that

$$R_{so} = \left(\frac{\overline{V_u^2}}{\overline{I_n^2}} + R_\gamma^2\right)^{1/2} \tag{5.12}$$

after a tedious bit of algebra we find

$$T_n = \frac{\overline{I_n^2}R_\gamma(1-|\rho_n|^2) + (\overline{V_u^2}\,\overline{I_n^2} + R_\gamma^2\overline{I_n^4})^{1/2}(1+|\rho_n|^2)}{2K(1-|\rho_n|^2)} \tag{5.13}$$

where $\rho_n = \rho_7$ is the "noise reflection coefficient," or reflection coefficient with respect to the "noise load" Z_n, in the general case. Of special note is the case for $R_\gamma = 0$, when

$$T_n = \frac{(\overline{V_u^2}\,\overline{I_n^2})^{1/2}(1+|\rho_n|^2)}{2K(1-|\rho_n|^2)} . \tag{5.14}$$

Consider now the network of Fig. 5.1(b), which consists of the same networks as in (a), except that the inner terminations have been removed and Terminals 4 of N_2 have been joined to Terminals 5 of N_3. Since the networks seen looking into Terminals 2, 4, 6, and 7 are unchanged, the corresponding impedances are unchanged. In general, however, the remaining impedances and all reflection coefficients, shown primed, will be different. We will denote by $|\rho_n|$ the magnitude of all ρ_i since they must be equal. Since

$$\rho_4 = \frac{Z_4 - 1}{Z_4 + 1} \tag{5.15}$$

$$\rho_5 = \frac{Z_5 - 1}{Z_5 + 1} \tag{5.16}$$

$$\rho_5' = \frac{Z_5 - Z_4^*}{Z_5 + Z_4} \tag{5.17}$$

we can solve for a bound on ρ_5' as a function of ρ_4 and ρ_5,

$$|\rho_n| = |\rho_5'| \leq \frac{|\rho_4| + |\rho_5|}{1 + |\rho_4||\rho_5|} \quad . \tag{5.18}$$

Since Network N_3 is realizable if

$$\int_0^\infty ln \left|\frac{1}{\rho_5}\right| \, d\omega \leq \pi\Omega_p \tag{5.19}$$

where Ω_p is the intrinsic bandwidth of the preamplifier "noise load," some typical values of which are shown in Table 4.1, we can now calculate the upper bound on theoretical system noise temperature as a function of operating bandwidth ω_c, antenna intrinsic bandwidth Ω_a, and preamplifier noise parameters $\overline{V_u^2}$, $\overline{I_n^2}$, and Z_γ (or their duals). First, define

$$\rho_a \triangleq \text{Max } |\rho_4| \tag{5.20}$$

$$\rho_p \triangleq \text{Max } |\rho_5| \tag{5.21}$$

where ρ_4 and ρ_5 are desired functions of ω which meet the conditions of Eqs. (5.5) and (5.19), respectively. Combining Eqs. (3.32), (5.13), (5.18), (5.20) and (5.21), the system noise temperature T_s is bounded by

$$KT_s \leq KT_r + \frac{\overline{I_n^2}R_\gamma}{2} + \frac{(\overline{V_u^2}\overline{I_n^2} + R_\gamma^2\overline{I_n^4})^{1/2}\,[(1+\rho_a^2)(1+\rho_p^2) + 4\rho_a\rho_p]}{2(1-\rho_a^2)(1-\rho_p^2)} = KT_0 + W\frac{\rho_a^2(1+\sigma)^2}{(1-\rho_a^2)(1-\sigma^2\rho_a^2)} \tag{5.22}$$

where $T_0 = T_r + T_{n0}$ is the minimum possible system noise temperature, $\sigma = \rho_p/\rho_a$, and W is an auxiliary noise parameter defined as

$$W \triangleq (\overline{V_u^2}\overline{I_n^2} + R_\gamma^2\overline{I_n^4})^{1/2} \tag{5.23}$$

or its dual.

Assuming that σ should be a constant to make optimum use of the restraints on ρ_a and ρ_p, it can be evaluated by considering the case of holding ρ_a and ρ_p constant at their optimum values over bandwidth ω_c from ω_1 to ω_2, and letting them equal unity outside the band. Then

$$\int_{\omega_1}^{\omega_2} \ln \frac{1}{\rho_a}\, d\omega = \omega_c \ln \frac{1}{\rho_a} = \pi\Omega_a \tag{5.24}$$

and

$$\int_{\omega_1}^{\omega_2} \ln \frac{1}{\rho_p}\, d\omega = \omega_c \ln \frac{1}{\rho_p} = \pi\Omega_p \quad . \tag{5.25}$$

Combining,

$$\sigma = \frac{\rho_p}{\rho_a} = \exp \frac{\pi(\Omega_a - \Omega_p)}{\omega_c} \tag{5.26}$$

is the optimum value.

To attack the inverse problem of determining the bandwidth within which a specified maximum noise temperature function $T_{s1}(\omega)$ can be maintained, we solve Eq. (5.22) for ρ_a

$$\rho_a^2 = \frac{1 + \sigma^2 + (1+\sigma)^2\beta - \{[1 + \sigma^2 + (1+\sigma)^2\beta]^2 - 4\sigma^2\}^{1/2}}{2\sigma^2} \tag{5.27}$$

where

$$\beta = \beta(\omega) \doteq \frac{W}{[KT_{s1}(\omega) - T_0]} \quad . \tag{5.28}$$

Evaluating (5.27) for $\sigma = 0 (\Omega_p - \Omega_a >> \omega_c)$

$$\rho_a^2(\sigma = 0) = \frac{1}{1+\beta} \tag{5.29}$$

and for $\sigma = 1 (\Omega_p = \Omega_a)$

$$\rho_a^2(\sigma = 1) = 1 + 2[\beta - (\beta^2 + \beta)^{1/2}] \tag{5.30}$$

Example 1: $\sigma = 0$, $T_{s\,l}$ constant from ω_1 to $\omega_1 + \omega_c$.

$$\int_{\omega_1}^{\omega_1+\omega_c} ln\ \frac{1}{\rho_a}\ d\omega = \frac{1}{2}\int_{\omega_1}^{\omega_1+\omega_c} ln\ (1+\beta)d\omega = \frac{\omega_c}{2}\ ln\ (1+\beta) \qquad (5.31)$$

and

$$\omega_c \leq \frac{2\pi\rho_a}{ln\ (1+\beta)} = \frac{2\pi\rho_a}{ln\left[1 + \dfrac{W}{K(T_{s\,l} - T_0)}\right]} \qquad (5.32)$$

or

$$T_{s\,l} \geq T_0 + \frac{W}{K\left[\exp\ \dfrac{2\pi\rho_a}{\omega_c} - 1\right]} = \eta T_0 \qquad (5.33)$$

The coefficient η is shown in Fig. 5.2 as a function of ω_c/ρ_a for several values of $(2KT_0/W)$ from 1, the lowest value it can have ($T_{n\,o} = \infty$); to 50, corresponding to $T_{n\,o} \approx 6°K$ for room temperature operation. The bandwidth advantage of low noise temperature is apparent.

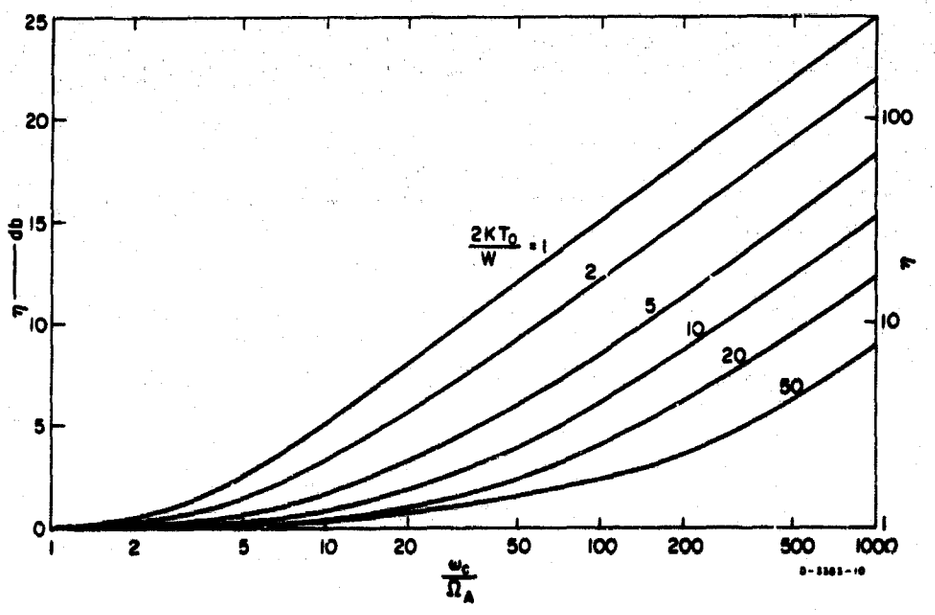

FIG. 5.2 SENSITIVITY LOSS vs. BANDWIDTH FOR FLAT REFLECTION COEFFICIENT

Example 2: $\sigma = 0$, $T_{s\ell} = T_0\ (\omega/\omega_0)$ for $\omega \geq \omega_1$.

The object of this example is to determine whether an infinite bandwidth is available above a given minimum frequency by allowing the system noise temperature to rise linearly with frequency (3 db per octave). For this case,

$$1 + \beta = \frac{\omega - \omega_0\left(1 - \frac{W}{KT_0}\right)}{\omega - \omega_0} \tag{5.34}$$

and

$$M = \int_{\omega_1}^{\infty} ln\ (1 + \beta)d\omega$$

$$= \left(\frac{\omega_1}{\omega_0}\right) ln\left(\frac{\omega_1}{\omega_0} - 1\right) - \left(\frac{\omega_1}{\omega_0} - 1 + \frac{W}{KT_0}\right) ln\left(\frac{\omega_1}{\omega_0} - 1 + \frac{W}{KT_0}\right) . \tag{5.35}$$

For the matching network to be realizable, M must be less than $2\pi\Omega_a/\omega_0$, which it is for certain values of ω_1/ω_0 and W/KT_0. In fact, it is realizable for $\omega_1/\omega_0 = 1$, or $T_s(\omega_1) = T_0$, for $\omega_1/\Omega_a \leq X(W/KT_0)$. While the function X has not been determined in general, it is about 17.2 for $W/KT_0 = 1/3$, a reasonable value for transistors. Furthermore, $T_s(\omega_1)/T_0$ rises so slowly for $\omega_1/\Omega_a > X$ that it can generally be ignored. For instance, for $W/KT_0 = 1/3$, $T_s(\omega_1 = 10X)/T_0 = 1.25$, or 1 db.

Now let us consider what these limits of noise temperature mean in terms of limiting the sensitivity of a receiving system using a small antenna, such as those described in Sec. 2. Defining E_0 as the (rms) electric field incident on a capacitive antenna which produces an output amplitude equal to the system noise in a 1-Hz bandwidth, we can set $P_s = P_n$ in Eq. (3.33), and find

$$P_{a0} = \frac{V_{s0}^2}{4R_s} = KT_s \tag{5.36}$$

Substituting into Eq. (2.22),

$$E_0^2 = \frac{4\Omega_a KT_s}{\omega^2 \varepsilon S} \tag{5.37}$$

Similarly for inductive antennas,

$$H_0^2 = \frac{4\Omega_a KT_s}{\omega^2 \mu S} \tag{5.38}$$

As a practical example, the threshold field strength E_0 for $\sigma = 0$, $T_{s\ell}$ constant in bandwidth ω_c is given by

$$E_0^2 = \frac{4\Omega_a}{\omega^2 \epsilon S}\left[KT_0 + \frac{W}{\exp\left(\frac{2\pi\Omega_a}{\omega_c}\right) - 1}\right] \tag{5.39}$$

which has its minimum value for $\omega_c = 0$

$$E_0^2(\omega_c = 0) \doteq E_{00}^2 = \frac{4\Omega_a KT_0}{\omega^2 \epsilon S} \tag{5.40}$$

and, in general,

$$E_0^2 = E_{00}^2 \eta$$

where η is defined in Eq. (5.33) and shown in Fig. 5.2. Several examples of theoretical threshold field strength, normalized to 1-Hz noise bandwidth and 1 m^3 effective volume, are illustrated in Fig. 5.3 as a function of frequency. These plots apply either to electric fields in free-space permittivity or to magnetic fields in free-space permeability, for noise parameters typical of a transistor preamplifier operating at room temperature. Except for the lines labeled E_{00}, which are the limiting values for small bandwidth, each line represents an example of the lower limit of broadband sensitivity when the passband is bounded by the vertical arrows. Arrows on the sloping lines indicate infinite extensions.

All light lines are for an intrinsic antenna bandwidth of 10 Hz, while heavy lines are for 1 kHz. The dotted line is the locus of E_{00} for a typical antenna system with 10-Hz intrinsic (low-frequency) bandwidth but maximum Q of 500 at 10 kHz. The examples parallel to E_{00} are for constant $T_{s\ell}$ and clearly show the effect of passband by their displacement from E_{00}. Among the 1-kHz intrinsic bandwidth curves, the one for the 0-to-10-kHz passband is about 2 db above E_{00}; for 10-to-30 kHz, 3 db; and for 0-to-100 kHz, 8 db. The 0-to-10 kHz passband with 10 Hz

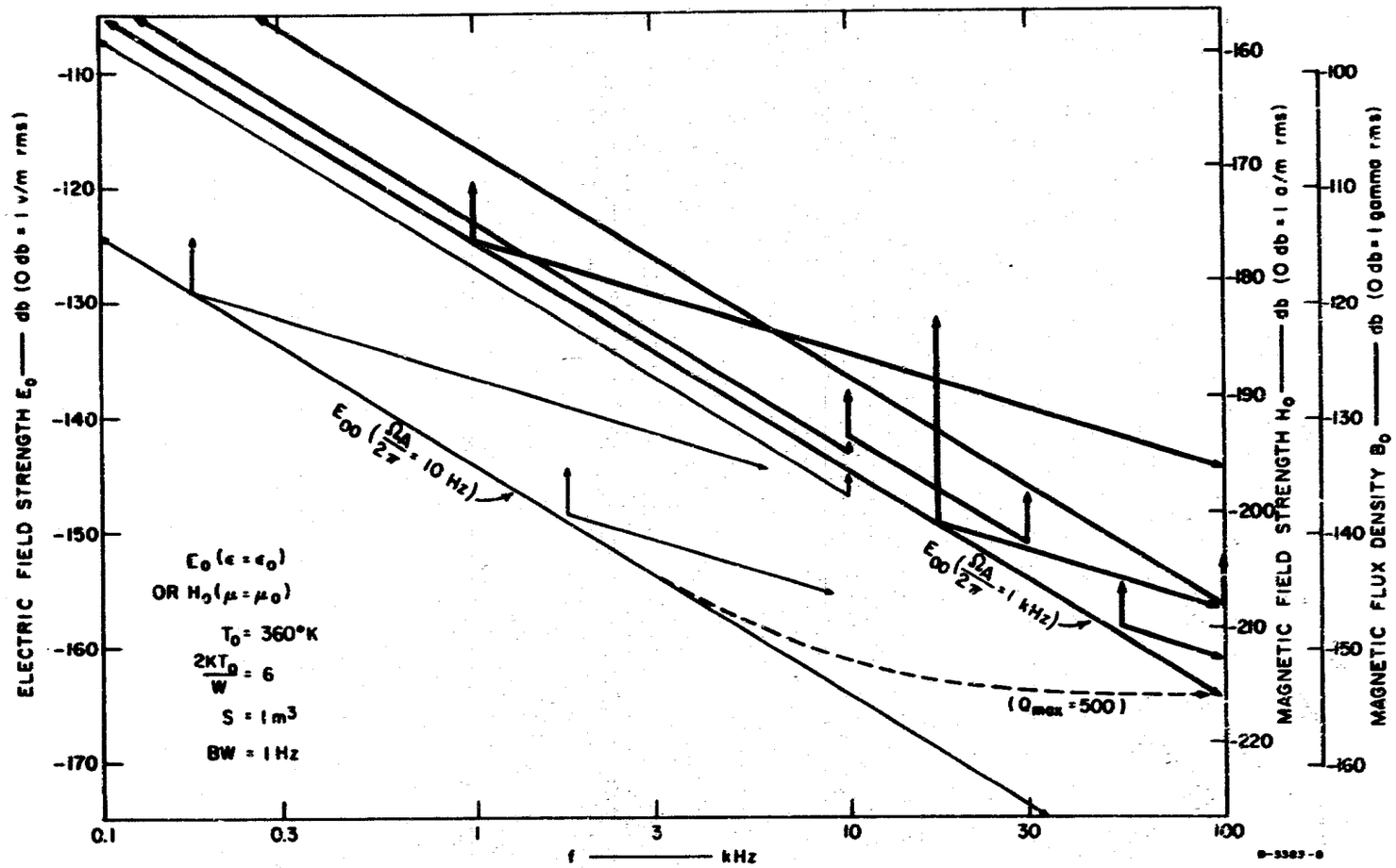

FIG. 5.3 THEORETICAL SENSITIVITY LIMITS

intrinsic bandwidth is 17 db above its E_{00}, or only 5 db below the same passband with 1-kHz intrinsic bandwidth. The lines of less slope represent possible sensitivity limits of the type in Example 2 above, where noise temperature is linear with frequency above a lower cutoff, shown by the vertical arrow. Although theoretically infinite, the passbands will be limited in practical cases by circuit Q.

BLANK PAGE

6. SUMMARY AND CONCLUSIONS

The basic difficulty in optimizing the noise performance of receiving systems which must use an electrically small antenna is the lack of a complete noise theory for a reactive source. This report has attempted to add to this theory in three areas:

First, the various types of small antennas have been put on a common basis of comparison. The parameters of effective length, effective area, effective volume, and intrinsic bandwidth have been defined for antennas sensitive to electrical fields and for those sensitive to magnetic fields. These parameters have been evaluated for a number of common antenna structures.

Second, a general method of describing the noise performance of any amplifier has been developed in both of its dual forms. This particular characterization, based on complex-correlated input noise voltage and current generators, was chosen out of many possibilities because it is easily applied to the problem of determining noise performance with an arbitrary source. These noise parameters have been evaluated for several types of amplifying devices.

Third, the ultimate theoretical limits on sensitivity have been explored, and a general method of determining the bounds, in terms of the parameters introduced in the previous sections, has been developed. These bounds have been evaluated in several examples.

While theoretical limits of sensitivity have been determined in this work, it has been assumed that an infinite number of lossless elements may be used in the matching network. In a practical application, an approximation to the desired reflection coefficient function must be found which will result in a physically practical network, a subject beyond the scope of this work except for a few general comments. For passbands that are not much wider than the intrinsic bandwidth of the antenna, very simple coupling networks, such as a single tuning element, will provide near-ideal performance. It is also apparent that as preamplifier noise temperature is lowered, the bandwidth avialable at a given sensitivity is increased or the number of elements necessary in the coupling network is

reduced. For this reason, as well as the ease with which its optimum source impedance can be adjusted, the parametric amplifier appears to warrant considerably more study.

It has also been shown that the magnitude of the optimum source impedance, assuming that its phase angle cannot be adjusted, is always the ratio of equivalent input short-circuit noise voltage to open-circuit noise current. This is extremely useful when complicated matching networks cannot be used, since these noise parameters are relatively easily measured. This observation also shows that, when simple coupling networks are required, preamplifiers with capacitive inputs, such as FET's or paramps, are inherently better suited to capacitive antennas than to inductive antennas. Conversely, an inherently inductive preamplifier, such as an inductive paramp, is needed to match inductive antennas.

Finally, some comments about the environment of the system are in order. For instance, if low-noise preamplifiers and efficient coupling networks are used, a large portion of the system noise may be due to loss resistance in the antenna system. Operation of the lossy elements at lower temperature will then improve sensitivity.

In many applications the limit of sensitivity will be set by external noise, such as sferics, precipitation static, or power-line harmonics. Since these are impulsive or periodic noises rather than Gaussian, they can be reduced by methods reported elsewhere. If the antenna is immersed in a conducting medium, however, irreducible noise sources may be added corresponding to the loss coupled into the antenna at the temperature of the medium. If the medium is a plasma, there will also be shot noise due to the random motion of charged particles in the vicinity of the antenna.

While the sensitivity limits derived are quite general, it must be pointed out that they are given in terms of the electric field and actual permittivity for capacitive antennas, and in terms of the magnetic field and actual permeability for inductive antennas. It is apparent that antennas can be constructed which will allow accurate measurement of any one of the four basic field quantities, or both quantities of one type if antenna impedance is also measured. Properly designed antennas of one type are, of course, relatively immune to fields of the opposite type. Shielded or single-turn small loops, for instance, are insensitive to electric fields; while plates and dipoles are insensitive to magnetic

fields. Relating electric to magnetic fields, or to propagating power density, requires independent knowledge of the propagation constants. Also, the proper value of ϵ or μ must be used in sensitivity calculations. This is particularly difficult for a capacitive antenna in a plasma, where ϵ is complex and variable. In addition, the existence of an ion sheath may alter the apparent ϵ and the actual sensitivity considerably.

BLANK PAGE

REFERENCES

Biard, J. R., "Low-Frequency Reactance Amplifier," *PROC. IEEE*, 51, 298-303 (February 1963).

Blackwell, L. A., and K. L. Kotzebue, *Semiconductor-Diode Parametric Amplifiers*, 9-13, 122-132 (Prentice-Hall, 1961).

Bode, H. W., *Network Analysis and Feedback Amplifier Design* (Van Nostrand, 1945).

Bruncke, W. C., "Noise Measurements in Field-Effect Transistors," *Proc. IEEE*, 51, 378-379 (February 1963).

Deaver, B. S. Jr., and W. S. Goree, "Cryogenic Magnetometer Development," Midterm Report for NASA Ames Research Center, Contract NAS 2-2088 (15 March 1965).

Fano, R. M., "Theoretical Limitations on the Broadband Matching of Arbitrary Impedances," *Franklin Institute*, 249, 57-83 (January 1950).

Haus, H. A., and R. B. Adler, "Circuit Theory of Linear Noisy Networks," (Wiley, 1959).

Harrington, R. F., "Time-Harmonic Electromagnetic Fields," 355-361 (McGraw Hill Book Co., Inc., 1961).

IRE Subcommittee 7.9 on Noise, "Representation of Noise in Linear Twoports," *Proc. IRE*, 48, 69-74 (January 1960).

Jordan, A. G., and N. A. Jordan, "Theory of Noise in Metal Oxide Semiconductor Devices," *IEEE Trans. ED*-12, 148 (March 1965).

Nielsen, E. G. "Behavior of Noise Figure in Junction Transistors," *Proc. IRE*, 45, 957-963 (July 1957).

Schelkunoff, S. A. and H. T. Friis, *Antennas, Theory and Practice*, 34-36, 302-329 (John Wiley and Sons, Inc., 1952).

Terman, Frederick Emmons, *Radio Engineers' Handbook*, 47-57, 112-118 (McGraw-Hill Book Co., Inc. 1943).

van der Ziel, A., *Noise* (Prentice-Hall, 1954).

van der Ziel, A., "Noise in Junction Transistors," *Proc. IRE*, 46, 1019-1038 (June 1958).

van der Ziel, A. "Thermal Noise in Field-Effect Transistors," *Proc. IRE*, 50, 1808-1812 (August 1962).